Available online at www.sciencedirect.com
SCIENCE DIRECT®
Electrochimica Acta 51 (2005) 1044–1058
ELECTROCHIMICA Acta
www.elsevier.com/locate/electacta

Combined voltammetry and in situ infrared spectroscopy of tetramethylthiourea on gold in aqueous acid solutions

A.E. Bolzán[a,*,1], T. Iwasita[b,1], A.J. Arvia[b,1]

[a] *Instituto de Investigaciones Fisicoquímicas Teóricas y Aplicadas (INIFTA) (UNLP, CONICET), Sucursal 4, Casilla de Correo 16, (1900) La Plata, Argentina*
[b] *Instituto de Quimica de São Carlos, Universidade de São Paulo, São Carlos, Brasil*

Received 28 January 2005; received in revised form 12 May 2005; accepted 31 May 2005
Available online 14 July 2005

Abstract

The voltammetric behaviour of tetramethylthiourea (TMTU) dissolved in aqueous perchloric and sulphuric acid solutions on polycrystalline gold combined with in situ Fourier transform infrared reflection absorption spectroscopy (FTIRRAS) was investigated. Conventional and triangular modulated voltammetry and rotating disc electrode data demonstrate the occurrence of two redox surface processes in the potential ranges $-0.1 \leq E \leq -0.3$ V and $0.7 \leq E \leq 0.8$ V (versus SHE), respectively. These processes would involve the participation of TMTU adsorbates. The redox surface process observed in the range -0.1 to -0.3 V can be related to the electrosorption of TMTU. The absence of infrared absorption bands from these adsorbates agrees with a flat, almost parallel adsorption of TMTU molecules on gold that has been already reported. In the range $0.4\,\text{V} \leq E \leq 0.8\,\text{V}$ both electrochemical and spectroscopic data indicate the anodic formation of soluble gold–TMTU complex and tetramethylformamidine disulphide ($TMFDS^{2+}$) ions presumably via $Au(TMTU)^{+}$ adsorbates. The kinetics of soluble gold–TMTU complex ion formation is under diffusion control, whereas the formation of $TMFDS^{2+}$ ions behaves as a rather irreversible process with the anodic slope, derived from current–potential curves, $\partial E/\partial \log I = 0.120\,\text{V decade}^{-1}$ at 298 K. At $E > 1.2$ V, the global electro-oxidation of both TMTU and $TMFDS^{2+}$ species yields carbon dioxide, sulphate ions and carbonyl-containing compounds, as indicated by IR spectra. These reactions involve the participation of oxygen-containing adsorbates produced from water electro-oxidation on gold.

Keywords: Tetramethylthiourea; Electro-oxidation; FTIRRAS; Gold; Electrodissolution

1. Introduction

The adsorption and electro-oxidation of thiourea (TU) and substituted thioureas are of much interest in metal electroplating as possible additives. [1–6]. On the other hand, at potentials sufficiently positive, these compounds likely act either as promoters for the electrodissolution of the base metal through the formation of soluble complex species [7] or produce insoluble films that to some extent impede metal corrosion [8]. Protective films of TU derivatives have been considered as possible corrosion inhibitors in nuclear reactors [9,10]. TU and TU derivatives, including tetramethylthiourea (TMTU), have also been considered as possible lixiviants for gold recovery from minerals [11–14] by electrodissolving gold via the formation of soluble complex species [15,16].

On the other hand, the similarity between TU and TMTU includes the formation of formamidinium disulphide (FDS^{2+}) and tetramethylformamidinium disulphide ($TMFDS^{2+}$), respectively, by homogeneous chemical oxidation in the presence of hydrogen peroxide [17,18] (Fig. 1).

According to capacitance measurements [19] the adsorption of TMTU on gold takes place in the range -0.25 to 0.8 V (versus the standard hydrogen electrode, SHE) and its desorption occurs at ca. 0.85 V (SHE). A substantial adsorption of TMTU has been inferred from the low and almost constant capacity of 10–13 $\mu\text{F cm}^{-2}$ measured in the range -0.25 to 0.8 V (SHE). Seemingly, the structure of the TMTU adsorbate depends on the nature of the metal electrode. Thus,

* Corresponding author. Tel.: +54 22 1425 7430; fax: +54 22 1425 4642.
E-mail address: aebolzan@inifta.unlp.edu.ar (A.E. Bolzón).
[1] ISE member.

0013-4686/$ – see front matter © 2005 Elsevier Ltd. All rights reserved.
doi:10.1016/j.electacta.2005.05.043

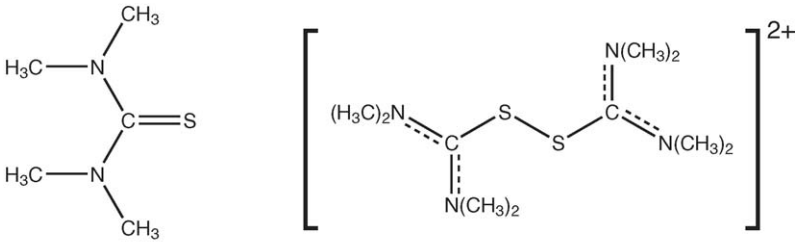

Tetramethylthiourea(TMTU) Tetramethylformamidinium disulphide(TMFDS)$^{2+}$

Fig. 1. Chemical structural formulas of TMTU and (TMFDS)$^{2+}$.

for mercury the surface excess of 3.3×10^{-10} mol cm^{-2} has been determined [20], whereas for Au (1 1 1) the surface excess decreases to 2.1×10^{-10} mol cm^{-2} [21]. Scanning tunnelling microscopy (STM) imaging indicates that TMTU molecules are likely lying almost flat on the gold surface with a slight tilt arising from the local spatial requirements of methyl groups [21]. The adsorption of TMTU on polycrystalline gold in both acid and base has also been investigated by SNIFTIRS [22]. From *p*- and *s*-polarised light spectra it has been concluded that the TMTU molecule adsorbs with the NCSN plane parallel to the electrode surface.

Likewise, at sufficiently positive potentials gold electrodissolution via the formation of a soluble gold–TMTU complex has been proposed [19,22], although neither IR nor X-ray diffraction data for this complex species have been reported, in contrast to TMTU complex species of several transition metals, such as Zn, Cd, Co, Pd, Pt and Pb [23], Se [24], Te [25] and Cu [26].

TMTU adsorption plays an important role in the initial stages of gold electrodissolution, as concluded from STM imaging [15,21]. Seemingly, single-crystal gold etching starts at step edges of the surface, eventually producing monoatomic steps oriented at 60/120° with respect to each other. At sufficiently negative potentials, TMTU-gold complex species can be electroreduced yielding gold islands by a nucleation and growth mechanism [15].

Previous electrochemical work has focussed mainly on either TMTU adsorption on gold [19,22] or TMTU-assisted electrodissolution of gold [15], with a rather scant regard for the complexity of the overall reaction and product formation. This fact encouraged us to investigate the electrochemistry of TMTU on polycrystalline gold electrodes, particularly its electro-oxidation, by combining in situ Fourier transformed infrared reflection-absorption spectroscopy (FTIRRAS) and voltammetric routines including triangular modulated and rotating disc electrode voltammetry. The results presented in this paper allow us to determine the potential ranges where various electrochemical reactions, such as the electrodissolution of gold, the formation of soluble TMFDS^{2+} species and the electro-oxidation of both TMTU and TMFDS^{2+} to oxygen-containing products, take place. Correspondingly, a possible electrochemical reaction pathway is advanced.

2. Experimental

2.1. Voltammetry

Voltammograms were run utilising a conventional three-electrode cell with a polycrystalline gold wire working electrode (0.25 cm^2 geometric area, J. Matthey, spec pure), a large platinum sheet (2 cm^2 geometric area) as counter electrode, and a mercurous sulphate electrode (MSE) as the reference. The working electrode was mechanically polished with alumina and rinsed with Milli-Q* water before each experiment. Triangular modulated (tm-) voltammetry was employed for visualising surface electrochemical processes occurring in the order of msec [27–30]. This technique consists of a triangular signal of frequency (f) and amplitude (A_m) that modulates a slow linear or triangular potential scan. The shape of the envelope of the current/potential display depends on f and A_m. Then, by properly adjusting f and A_m, the optimal coupling between the modulating signal and the rate of the electrochemical reaction can be estimated. For all these measurements, an LYP potentiostat coupled to a waveform generator was employed.

Current/potential curves were also measured utilising a rotating gold disc electrode (0.12 cm^2 geometric area), a Tacussel type EAD 10 K rotating gold disc, a platinum sheet counter electrode of about 2 cm^2 and a Voltalab 10 Radiometer potentiostat.

2.2. FTIRRAS

For in situ FTIRRAS a Nicolet Nexus 670 spectrometer equipped with a liquid nitrogen-cooled MCT detector was used. The spectroelectrochemical cell was fitted with a 60° prismatic calcium fluoride window. The working electrode was a gold disc 0.7 cm in diameter that prior to each run was mechanically mirror-polished with alumina 0.3 μm grit and rinsed with Milli-Q* water. A reversible hydrogen electrode (RHE) was used as the reference and a gold foil surrounding the working electrode was employed as counter electrode. The working electrode potential was monitored by means of a Wenking 72 L potentiostat coupled to a potential step generator.

Normalised reflectance spectra were expressed as the ratio R/R_0, where R is the value of the reflectance at the

sampling potential E_S and R_0 is the reflectance measured at the reference potential E_{ref}. The value of E_{ref} was set at 0.05 V, a potential where TMTU electro-oxidation is precluded, and the potential was either decreased down to −0.2 V or increased up to 1.6 V in 0.05 V steps. Occasionally, the electrode was immersed in the working solution and held at $E_{ref} = 0.05$ V, i.e., a potential sufficiently positive for producing an incipient electro-oxidation of TMTU. Subsequently, the potential was decreased stepwise to −0.2 V and the electroreduction of the soluble products formed during the initial TMTU electro-oxidation stage on gold was followed by FTIRRAS.

Positive- and negative-going absorption bands in the spectra represent the loss and gain of species at E_S as compared to E_{ref}, respectively. At E_S, 256 interferograms with 8 cm^{-1} resolution were computed. Parallel (*p*) and perpendicular (*s*) polarised light was obtained from a barium fluoride-supported aluminium-wire grid polariser. Deuterium oxide solutions were also employed to study IR spectra in the region where water bands may obscure the presence of those related to TMTU and its oxidation products as well.

FTIRRAS flow cell experiments were made to study the electro-oxidation of TMTU adsorbates on gold. The cell was filled with ca. 7 ml of aqueous 0.1 M TMTU + 0.1 M $HClO_4$ and the gold electrode held at 0.05 V for 300 s. Then, the working electrode was pulled up few millimetres to assist the replacement of the solution between the electrode and the prismatic window, while maintaining the gold electrode at constant potential. Then, the TMTU-containing solution was fast and exhaustively replaced by flowing 200 ml of plain aqueous 0.1 M $HClO_4$. Subsequently, the working electrode was put once again in contact with the prismatic window to record a reference spectrum at $E_{ref} = 0.05$ V. Afterwards, E was stepped to either 1.2, 1.5 or 1.6 V to electro-oxidise strongly bound residues, recording the corresponding spectra. In this case, to increase the sensitivity of the signal, 1000 interferograms using *p*-polarised light were collected.

2.3. Solutions

Working solutions were prepared from TMTU (Fluka, puriss.), sulphuric acid (98% Mallinckrodt AR), perchloric acid (70% Alfa Aesar) and either Milli-Q* water or deuterium oxide (Aldrich, 99.9%). Solutions were kept under nitrogen saturation during the experiments.

Runs were made at room temperature and potentials in the text are referred to the SHE scale.

3. Results

3.1. Voltammetry

A stabilised cyclic voltammogram of polycrystalline gold in aqueous 1 mM TMTU + 0.1 M perchloric acid run at 0.05 V s^{-1}, between 0.05 and 0.95 V (Fig. 2a, full trace), shows an anodic current peak at 0.65 V (peak Ia) in the positive potential scan, and a cathodic peak at 0.36 V (peak Ic), preceded by a small hump at ca. 0.6 V, in the reverse scan. The equilibrium potential for the redox couple associated

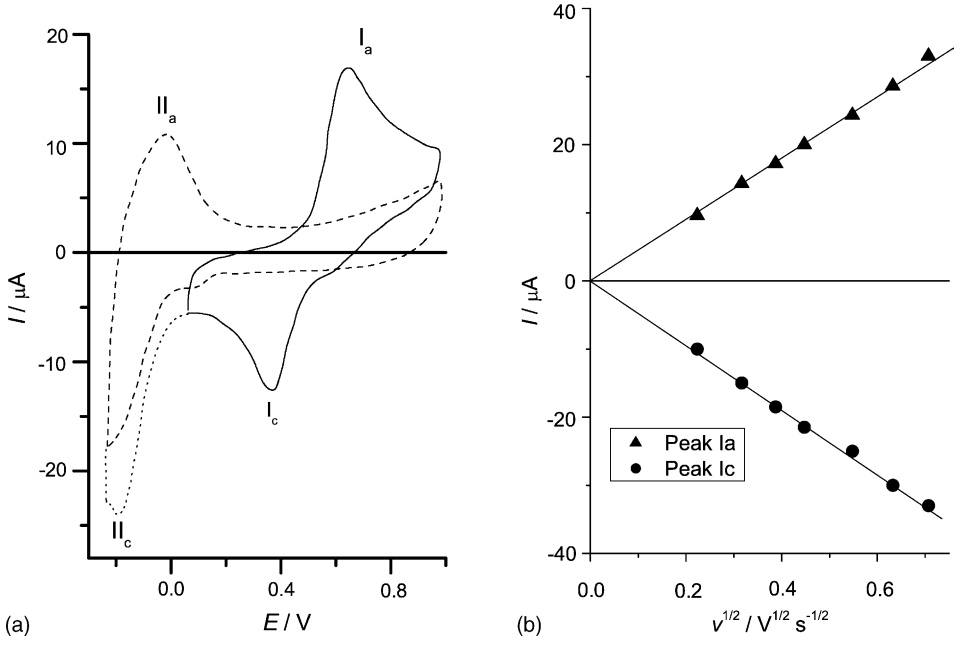

Fig. 2. (a) Voltammograms of gold in 1 mM TMTU + 0.1 M perchloric acid run at 0.05 V s^{-1}. Full line: stabilised profile between 0.05 and 0.95 V; dotted line: first cycle after decreasing the negative switching potential to −0.24 V; dashed line: stabilised profile run between −0.24 and 0.95 V. (b) Dependence of the height of current peaks Ia and Ic on $v^{1/2}$ after baseline correction from stabilised voltammetric data obtained between 0.05 and 0.95 V.

with peaks Ia/Ic is close to 0.47 V, i.e. a value at which the anodic and cathodic current densities become equal. The voltammogram depicted in Fig. 2a reminds that related to the TU/formamidinium disulphide redox couple on different metals [7,31,32]. It should be noted that the voltammetric oxidation of TMTU on platinum also shows a similar conjugated pair of peaks, although in this case they appear only after a prolonged potential cycling [33].

As the negative potential limit (E_{cs}) is diminished from 0.05 to −0.24 V (Fig. 2a, dotted trace) and the positive potential limit (E_{as}) is maintained at 0.95 V, the voltammogram shows a new pair of conjugated peaks at ca. −0.024 V (peak IIa) and −0.18 V (peak IIc). As the potential cycling is restricted to the range −0.24 to 0.95 V, the height of peak IIc decreases and at ca. 0.1 V a hump appears. Simultaneously, the heights of peaks Ia and Ic gradually decrease and eventually disappear (Fig. 2a, dashed line). However, as E_{cs} is reset to 0.05 V, the pair of peaks Ia/Ic shows up again. This behaviour can be related either to the electrodesorption of TMTU or to the partial electroreduction of TMTU at low potentials, yielding residues that remain on the gold surface. These residues would be responsible for the disappearance of the pair of peaks Ia/Ic.

The height of peaks Ia and Ic depends linearly on $v^{1/2}$ with nearly similar anodic and cathodic slopes (Fig. 2b). This dependence is consistent with an electrochemical reaction under diffusion control [34].

When $E_{cs} = 0.05$ V and E_{as} is stepwise increased from 0.55 upwards (Fig. 3), as soon as the potential of peak Ia is exceeded the reversibility of the redox couple Ia/Ic decreases with E_{as}, and the contribution of the electrochemical process associated with the current hump preceding peak Ic emerges. Correspondingly, the cathodic current contribution following peak Ic commences to increase. These features indicate that at least two different electrochemical processes occur in the potential range 0.4–1.0 V. As we shall see later, these processes are the dissolution of gold as gold–TMTU complex ions and the formation of $TMFDS^{2+}$ soluble species.

Otherwise, when E_{as} is increased to 1.43 V, the pair of peaks Ia/Ic is also suppressed (Fig. 3). The voltammogram in the positive potential scan shows the anodic hump IIIa at ca. 1.25 V and a current peak at ca. 1.5 V (peak IVa). Likewise, the reverse scan exhibits peak IIIc at ca. 1.1 V related to the electroreduction of the oxygen-containing layer formed on gold during the preceding scan [35].

Therefore, as the potential scan is extended either negative to −0.24 V (Fig. 2a) or positive to 1.6 V (Fig. 3) peaks Ia/Ic are prevented. This effect might be due to the presence of an inhibitor for those reactions related to peaks Ia and Ic. This inhibitor appears to be produced on the electrode surface at either high negative or high positive switching potentials. This response is comparable to that previously reported for the electro-oxidation of TU on gold [31]. It suggests that the electro-oxidation reaction pathway of TMTU and TU on gold would be formally similar.

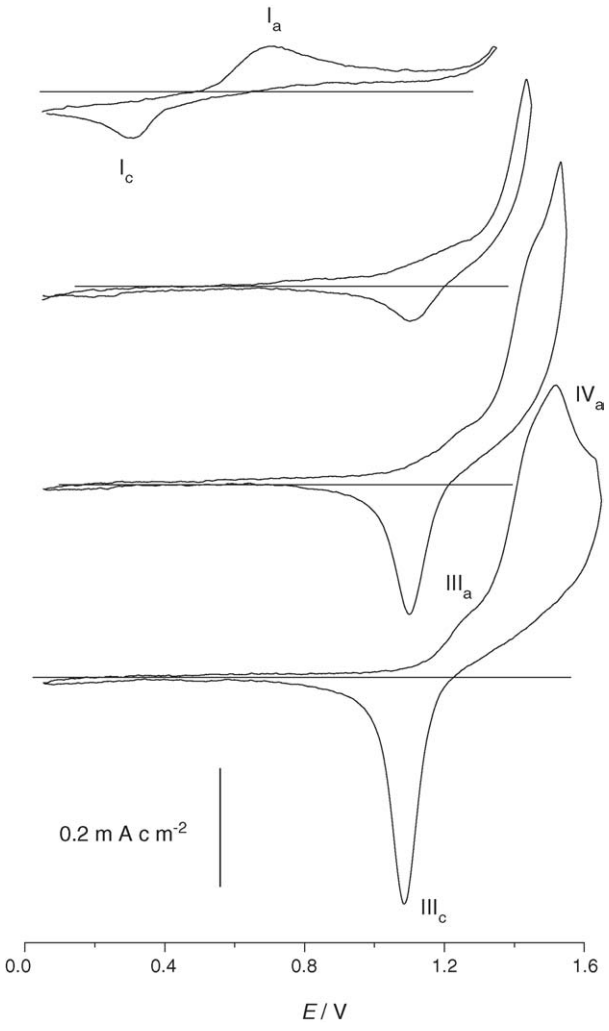

Fig. 3. Waterfall plot showing the voltammetric response of gold in 1 mM TMTU + 0.1 M perchloric acid at $v = 0.05\ V\ s^{-1}$ and different positive switching potentials.

3.2. Triangular modulated voltammetry

The triangular modulated voltammogram of gold in 1 mM TMTU + 0.1 M perchloric acid run at $0.5\ V\ s^{-1}$, $A_m = 0.040$ V and $f = 1$ kHz (Fig. 4) displays a voltammetric envelope with a capacitance contribution of ca. $5 \pm 1\ \mu F\ cm^{-2}$, two pairs of conjugated current peaks at ca. −0.15 (peak IIa/IIc) and 0.85 V (peaks Ia/Ic), and a small anodic peak at ca. −0.2 V (peak IIIa). The pseudocapacity value is in the range 10–13 $\mu F\ cm^{-2}$, in good agreement with capacitance data reported elsewhere [22].

For the pairs of peaks Ia/Ic and IIa/IIc anodic and cathodic charges are symmetrically distributed with respect to the baseline current, as expected for a rather fast redox surface reaction [30]. The pair of peaks IIa/IIc in Fig. 2 can be associated with the electroadsorption/electrodesorption of TMTU species. The electrodesorption process is coupled with the partial inhibition of TMTU electro-oxidation

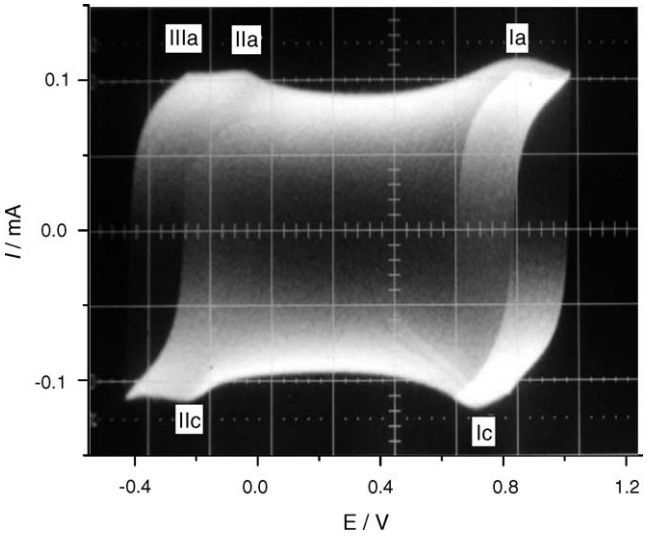

Fig. 4. Triangular modulated voltammogram of gold in 1 mM TMTU + 0.1 M perchloric acid; $v = 0.5\,\mathrm{V\,s^{-1}}$, $A_m = 0.04\,\mathrm{V}$, $f = 1\,\mathrm{kHz}$.

(peaks Ia/Ic, Fig. 2a). This effect is presumably caused by some residual sulphur-containing species formed at $E < 0.1\,\mathrm{V}$.

The second surface electrochemical process at ca. 0.95 V lies close to the potential related to the first stage of the TMTU electro-oxidation reaction (peak Ia) in the voltammetric runs at $0.05\,\mathrm{V\,s^{-1}}$ (Fig. 2a). According to tm-voltammetry data, this reaction also involves a first relatively fast electron transfer step.

3.3. Voltammetry at the rotating disc electrode

A voltammogram run at $v = 0.05\,\mathrm{V\,s^{-1}}$ and $\omega =$ 2000 rpm between 0.05 and 0.95 V (Fig. 5a, full trace) shows anodic and cathodic current waves as those found for an electrochemical reaction under mass transport control [34]. Solution stirring turns peak Ia into a limiting anodic current I_L accompanied by the disappearance of peak Ic, as soluble electro-oxidation products are swept out from the electrochemical interface.

When E_{cs} is decreased to $-0.24\,\mathrm{V}$ (Fig. 5a, dashed line), the pair of peaks IIc/IIa is observed. No influence of solution stirring on the height of peaks IIa/IIc is noticed, in agreement with tm-voltammetry data, i.e., the contribution of surface electrochemical reactions. At the same time, when E_{cs} is shifted from 0.05 V to $-0.24\,\mathrm{V}$, both peak Ia (Fig. 2a) and the anodic limiting current I_L (Fig. 5a) disappear, i.e., the electrochemical reaction related to peak Ia is strongly inhibited probably because of the formation of surface residues at $E < 0\,\mathrm{V}$. On the other hand, the linear dependence of I_L on $\omega^{1/2}$ with a positive ordinate at $\omega = 0$ (Fig. 5b) would indicate the contribution of an activated electrochemical process to the global reaction [34].

The diffusion coefficient (D) of reactants related to the convective-diffusion contribution in Fig. 5b was roughly estimated from the Levich equation for the RDE [34]. Thus, considering 2 electrons per mole of reactant, the reactant concentration $10^{-6}\,\mathrm{mol\,cm^{-3}}$ and the kinematic viscosity of solution ca. $0.01\,\mathrm{cm^2\,s}$, it results in $D \simeq 2.7 \times 10^{-6}\,\mathrm{cm^2\,s^{-1}}$. This figure is consistent with a solvodynamic radius of a

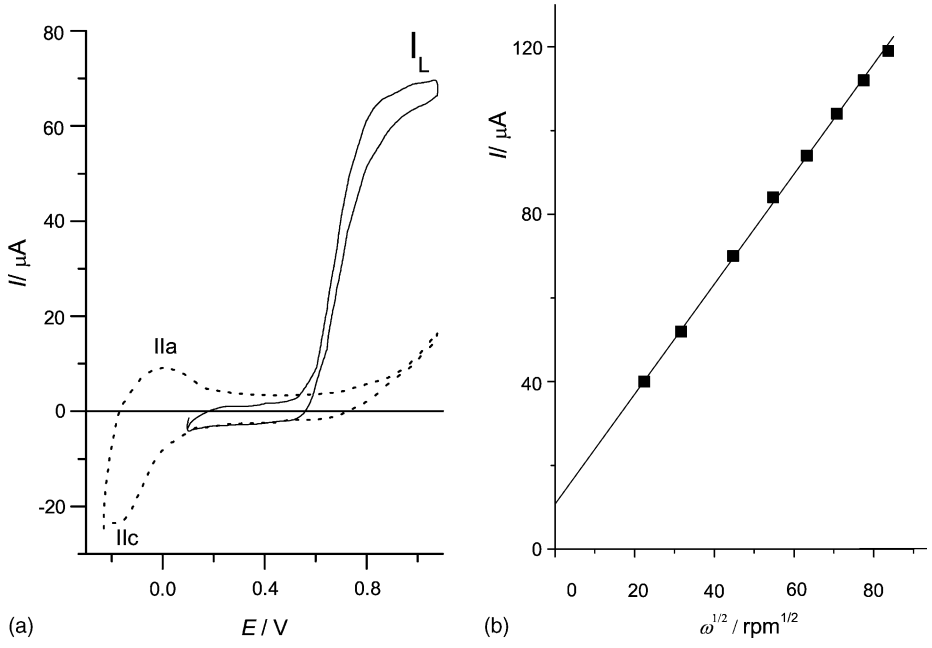

Fig. 5. (a) RDE voltammograms of gold in 1 mM TMTU + 0.1 M perchloric acid run at $0.05\,\mathrm{V\,s^{-1}}$ between 0.05 and 0.95 V (full line) and -0.24 and 0.95 V (dotted line), $\omega = 2000$ rpm. (b) Dependence of the RDE anodic limiting current recorded at $v = 0.005\,\mathrm{V\,s^{-1}}$ on $\omega^{1/2}$.

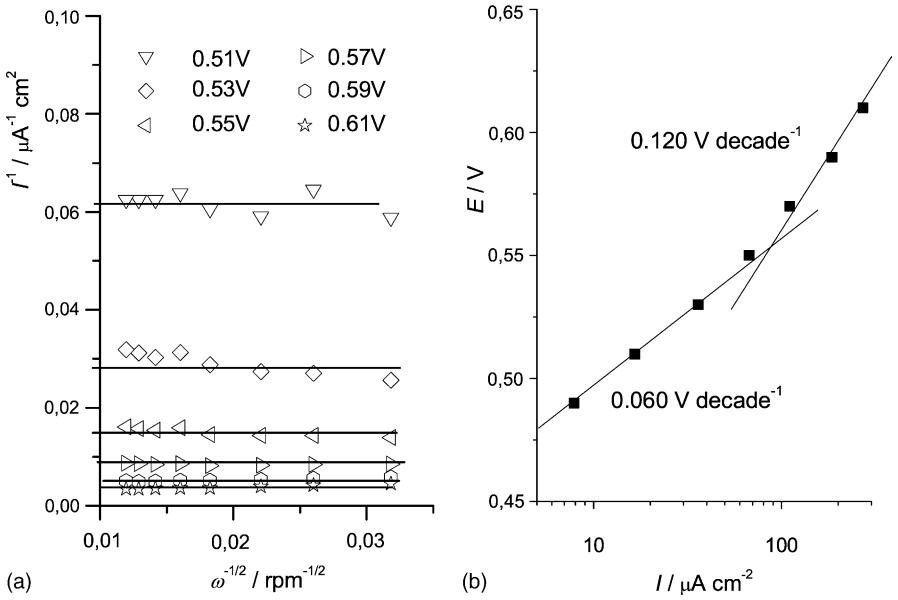

Fig. 6. (a) Plot of reciprocal anodic current from the rising part of the RDE voltammetric curve vs. the reciprocal RDE speed at different potentials; $v = 0.005$ V s^{-1}. (b) Tafel plot from data taken from (a), 1 mM TMTU + 0.1 M perchloric acid. The two limiting slopes are indicated.

diffusing species higher than that of TU in the same solutions [32,36].

At constant E, the rising part of the RDE voltammetric curve for $E > 0.49$ V, plotted as I^{-1} versus $\omega^{-1/2}$ (Fig. 6a), shows that I^{-1} becomes independent of ω. The kinetic current contribution, I_k, resulting from I^{-1} extrapolation to $\omega \to \infty$, fits an E versus log I_k linear plot with two limiting slopes, namely, $\Delta E/\Delta \log I_k = 0.060$ V decade^{-1} for $E < 0.55$ V and 0.120 V decade^{-1} for $E > 0.55$ V (Fig. 6b). The change in slope indicates a transition in the dominant electrochemical reaction in going from $E < 0.55$ V to $E > 0.55$ V. Presumably the kinetics and mechanism of each overall reaction are changing as well.

3.4. Voltammetric electro-oxidation of adsorbed TMTU

To confirm that surface species are formed on gold at potentials below that of peak Ia, a gold electrode was first immersed in either 0.1 or 1 mM TMTU-containing solution at 0.05 V for 300 s, then removed from the solution at constant potential and subsequently immersed in 0.1 M perchloric acid to run a voltammogram at 0.05 V s^{-1} from 0.05 V upwards. These voltammograms (Fig. 7) indicate that the threshold potential for TMTU adsorbate electro-oxidation is close to that where the oxygen-containing layer is formed [35]. The anodic peak at ca. 1.4 V is the same as that shown in Fig. 3, and the electro-oxidation charge ratio from comparable runs made in the presence (q_a) and in the absence (q_0) of TMTU results in $q_a/q_0 = 1.56$. This figure, which is obtained from the first positive scan, involves about 90% of the adsorbed TMTU monolayer on gold. Probably, because TMTU electro-oxidation on gold is accompanied by the formation of some

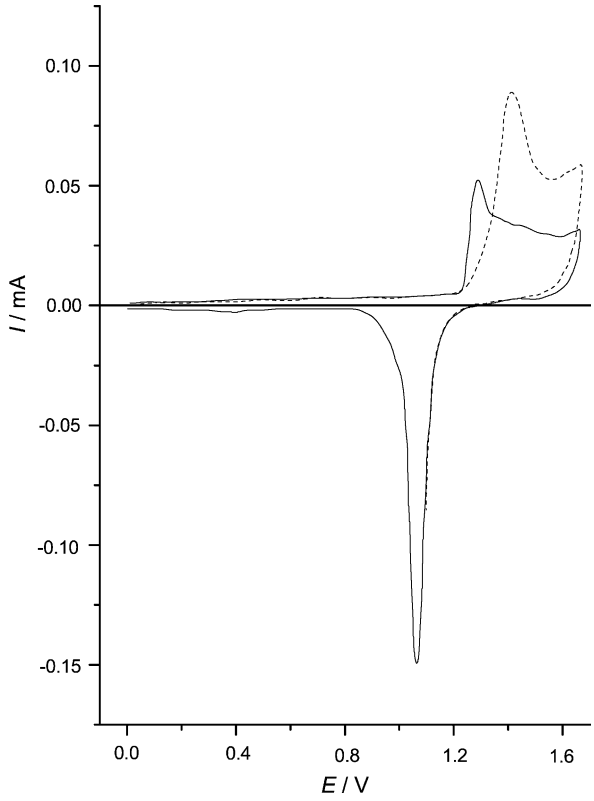

Fig. 7. First cycle for the voltammetric electro-oxidation of the TMTU adsorbate at $v = 0.05$ V s^{-1} in 0.1 M perchloric acid (- - -). TMTU was previously adsorbed on gold at 0.05 V for 300 s from aqueous 0.1 mM TMTU + 0.1 M perchloric acid, blank (—).

strongly bound carbonaceous residues, the complete adsorbate removal requires several potential cycles between 0.05 and 1.65 V. Nevertheless, the contribution of the oxygen-containing layer (q_{ox}) from water electro-oxidation remains almost the same, irrespective of adsorbed TMTU. Consequently, the difference $q_a - q_{ox} = 0.688\,mC\,cm^{-2}$ derived from the first electro-oxidation scan can be assigned to the electro-oxidation charge of TMTU adsorbates on gold.

3.5. FTIRRAS of gold in aqueous 0.1 M TMTU + 0.1 M perchloric acid

FTIRRAS measurements were performed in aqueous 0.1 M perchloric acid containing either 1 mM or 0.1 M TMTU. Spectra were obtained by setting $E_{ref} = 0.05$ V and collecting spectra by increasing the potential 0.05 V stepwise from E_{ref} to 1.5 V, utilising either *p*- or *s*-polarised light. To follow possible changes in the interface due to either the adsorption or the electroreduction of TMTU at low potentials, the value of E was also decreased stepwise from $E_{ref} = 0.05$ V to −0.2 V and back to 0.05 V.

Although several IR studies of TMTU have been reported [24,37–41], there are still some ambiguities concerning the assignments of bands. The spectrum analysis depends on whether each CH_3 group is considered as a single or a four-atom body, i.e., the molecule is considered as consisting of either 8 or 20 atoms [38,41]. The latter has been chosen for the analysis of SNIFTIRS data of the Au (1 1 1)| aqueous TMTU solution interface [19,21] and adopted in our work for the interpretation of spectral data. Considering that the IR spectrum of TMTU is complex because of the 54 normal vibration modes of the TMTU molecule, most of them being strongly coupled, only the strongest bands were considered (Table 1).

For the range $0.1 \leq E \leq 0.45$ V, the FTIRRAS spectra exhibit no significant changes, but for $E = 0.5$ V, a number of small negative and positive bands were found, their intensity increasing with E (Fig. 8). The appearance of these bands occurs when the current suddenly increases. Accordingly,

Table 1
Principal infrared bands of TMTU (taken from ref. [41])

Frequency	Assignment
1096 (s)	ρ CH_3, ν_aNCN
1119 (s)	ρ CH_3, νNCN
1131 (s)	ρCH_3
1150 (m)	δ_a CH_3NC,$\delta_a CH_3NCH_3$
1208 (m)	ρCH_3, $\nu_{as}CH_3$-N, ν_{as}NCN
1262 (s)	$\nu_s CH_3N$,ν_sNCN,ρCH_3
1360 (vs)	ν_{as} NCH_3, δ CH_3
1369 (s)	δ CH_3, ν_{as}NCN, $\nu_{as}NCH_3$
1403 (m)	$\delta_a CH_3NC$,$\delta_a CH_3NCCH_3$
1433 (m)	νCS,$\delta_s CH_3NC$,$\nu_a CH_3N$
1440 (m)	$\delta_a CH_3$
1470 (m)	$\delta_a CH_3$
1490 (m)	δCH_3,$\delta_a CH_3NC$,$\delta_a CH_3NCH_3$
1508 (s)	ν_sCN, ρCH_3, νCS

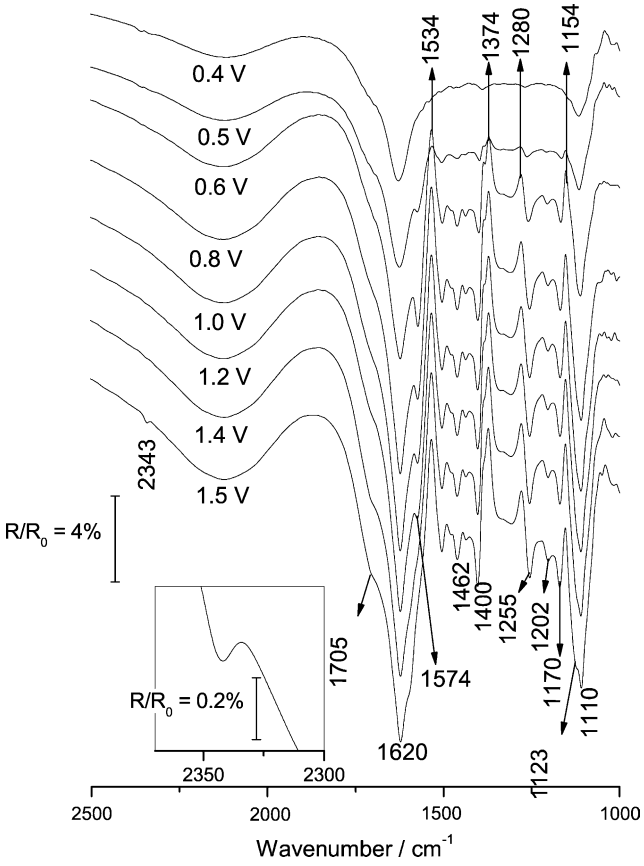

Fig. 8. *p*-Polarised light FTIRRAS spectra for the electro-oxidation of TMTU on gold in 0.1 M TMTU + 0.1 M perchloric acid at different sampling potentials, $E_{ref} = 0.05$ V.

electrochemical reactions involving TMTU start to be noticeable at near 0.5 V (Fig. 2a). Moreover, when $E > 0.8$ V, a strong yellow hue appears in the solution indicating a marked gold electrodissolution at these potentials, in agreement with voltammetric results.

At 0.55 V (Fig. 8) strong positive bands at 1154, 1280, 1374 and 1534 cm^{-1} and medium or weak bands at 1386, 1447 and 1489 cm^{-1} are observed. From Table 1 it is clear that these bands are related to the disappearance of TMTU from the thin solution layer. Simultaneously, negative bands at 1110, 1170, 1265, 1400, 1462, 1574 and 1620 cm^{-1} indicate the formation of new species from TMTU electro-oxidation, as discussed further on.

The assignment of negative bands becomes more complicated because of the scarce available spectroscopic information about TMTU-derivatives, particularly soluble gold complex species of the type $[Au(TMTU)_n]^+$. IR data of TMTU complexes have been reported for metals such as Zn, Cd, Co, Pd, Pt and Pb [23], Se [24], Te [25] and Cu [26]. For Se(II)-TMTU complexes the NCN antisymmetric stretching shifts from 1535 to 1585–1590 cm^{-1} [24] and for TMTU complexes with Zn, Cd, Co, Pd, Pt and Pb halides the blue shift from 1504 to 1542–1600 cm^{-1} is accompanied by a red shift of the CS stretching band from 1125 to

1098–1108 cm^{-1} [23]. These shifts are consistent with the formation of sulphur bridges between TMTU and the metal, increasing the double character bond between nitrogen and carbon, and simultaneously decreasing the double character bond between the carbon and sulphur atoms. SNIFTIRS data for Au (1 1 1) electrodissolution assisted by TMTU in aqueous acids show a band at 1571 cm^{-1} that has been assigned to gold–TMTU complex ions [15]. Therefore, the negative bands at 1573 and 1108 cm^{-1} can tentatively be assigned to the formation of soluble $[Au(TMTU)_n]^+$ ions.

The negative band at 1574 cm^{-1} appears concomitantly with a broad negative band at 1110 cm^{-1}. The latter lies close to the wavenumbers that have been assigned to the CS stretching band in TMTU complexes (1098–1108 cm^{-1}) [23,38,39]. In our case, the band at 1100 cm^{-1} might be somewhat obscured by the stretching band of perchlorate ions [42], as the concentration of the latter in the thin layer of solution increases gradually with E due to anion migration inwards to balance the formation of positively charged gold–TMTU complex ions and protons. The latter are produced from 1.2 V upwards due to water electro-oxidation yielding an oxygen-containing layer adsorbed on gold [35]. To avoid the interference of perchlorate ions, spectra were also run in sulphuric acid-containing deuterium oxide solutions, as described later on.

The negative band at 1620 cm^{-1}, which increases with E and progressively overlaps the band at 1573 cm^{-1}, is coupled with a gradual increase of the negative bands at 1400 and 1255 cm^{-1} and the appearance of a small feature at ca. 1700 cm^{-1}. The latter might be related to vestiges of CO-containing species produced from electro-oxidation side reactions of TMTU [33]. This is not surprising if one considers that this band appears for $E > 1.4$ V, i.e., a potential range where water electro-oxidation on gold takes place [35]. As the extinction coefficient of bands from CO-containing molecules is usually large, the yield of the corresponding reaction should be rather low. For $E \geq 1.4$ V, both a negative band at ca. 1202 cm^{-1} and a feature at 1123 cm^{1} are observed, the latter largely overlapping the band at 1110 cm^{-1}.

For $E > 1.4$ V, the negative bands at 1123 and 1202 cm^{-1} (Fig. 8) are related to the formation of sulphate and bisulphate ions, respectively [43], resulting from the complete electro-oxidation of TMTU. This reaction also yields carbon dioxide that is characterised by the small negative band at 2343 cm^{-1} (Fig. 8). The simultaneous formation of sulphate ions and carbon dioxide is likely assisted by OH and O surface species produced from water electro-oxidation. The electrochemical behaviour of TMTU for $E > 1.4$ V is to some extent comparable to that of TU on gold [44]. However, for TMTU, at variance with TU [44], no absorption bands related to the formation of CN-containing species are found. This means that CH_3 groups in the TMTU molecule impede the formation of the C≡N bond during the electro-oxidation reaction. The overall TMTU electro-oxidation reaction also implies the formation of nitrogen that is undetectable by FTIRRAS.

The *s*-polarised light spectra display the same bands reported above for *p*-polarised light spectra. Therefore, the above-discussed bands are related to either the formation of products or the depletion of reactants from the thin solution layer. The lack of bands related to adsorbed species confirms an earlier interpretation of SNIFTIRS data [22] considering that the strongest bands of TMTU involve skeletal stretching and deformations giving rise to large changes in the dipole moment on the plane of the NC(S)N skeleton. For the TMTU molecule adsorbed almost parallel to the metal surface, these changes will not contribute to IR spectra.

As the tm-voltammetry showed electrosorption current peaks for $E < 0.0$ V, spectra were also recorded by decreasing stepwise E from 0.05 to −0.2 V and then increasing it back to 0.05 V, in order to detect changes in the interface due to either the possible electroreduction of TMTU or the formation of electroadsorbed species (Fig. 9). Thus, as E is moved negatively, the corresponding spectra exhibit a small negative band at 1372 cm^{-1}. The intensity of this band slightly increases as E is shifted negatively (Fig. 9a), but when $E = -0.15$ V, the splitting of this band occurs and a new feature at ca. 1382 cm^{-1} is recorded. Unfortunately,

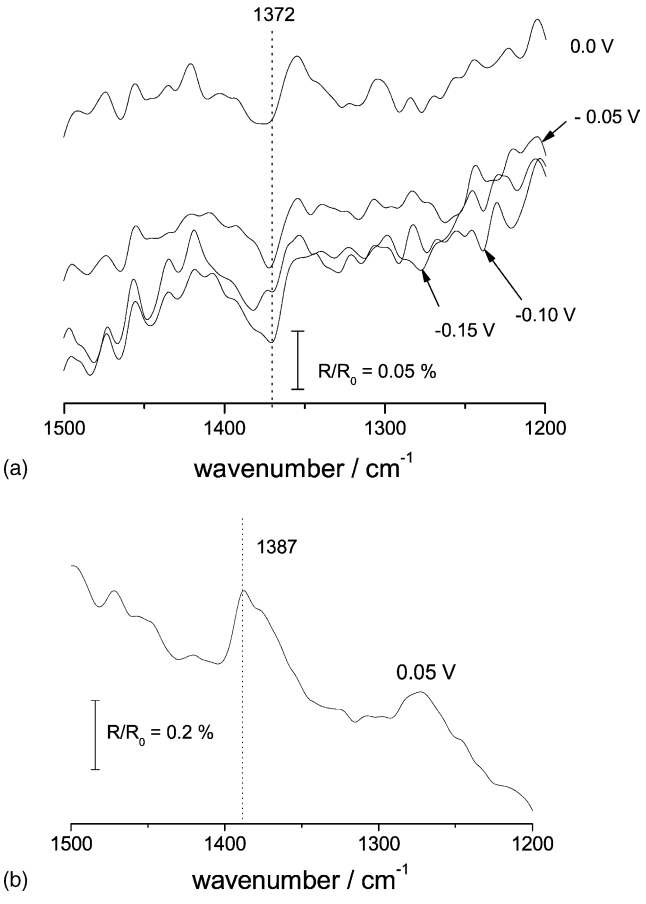

Fig. 9. (a) *p*-Polarised light FTIRRAS spectra for TMTU on gold in 0.1 M TMTU + 0.1 M perchloric acid at different negative sampling potentials. $E_{ref} = 0.05$ V. (b) Spectrum obtained after returning from −0.2 V to $E_{ref} = 0.05$ V.

the noise prevents the observation of any band displacement with E as expected for the presence of adsorbates. Furthermore, as E is reset to 0.05 V (Fig. 9b), the small positive band at 1387 cm^{-1} indicates that some species formerly present in the thin solution layer at E_{ref} have been consumed. The low intensity of all these bands and the changes operating in the spectra when E is moved from 0.05 to −0.2 V would be due to the electrodesorption of TMTU accompanied by the electroreduction of protons at these potentials.

After stepping E from −0.2 back to 0.05 V, the positive band recorded at 1387 cm^{-1} indicates that the local concentration of TMTU has decreased with respect to the initial one (Fig. 9b). This effect can be attributed to a possible electroreduction of TMTU to SH-containing species and the partial desorption of the latter.

In fact, for $E \leq -0.05$ V, the low intensity negative band at 2580 cm^{-1} (Fig. 10a) is in the spectral region corresponding to the S–H bond stretching [45]. The intensity of this band increases as E is decreased (Fig. 10b), suggesting an accumulation of electroreduced TMTU residues resulting from the interaction of adsorbed TMTU and hydrogen. The presence of these residues prevents the electrochemical process related to peak Ia (Fig. 2). The intensity of the band at 2580 cm^{-1} would be limited by the low concentration of hydrogen atoms on the gold electrode surface [46,47].

3.6. FTIRRAS in deuterium oxide solutions

As the band at 1620 cm^{-1} assigned to the formation of $TMFDS^{2+}$ might be obscured by the bending band of water at ca. 1640 cm^{-1} [42], to diminish the interference of water from the acid and to discriminate the CS stretching band of the gold–TMTU complex from the stretching band of perchlorate ion, spectra were also run in 0.1 M TMTU + 0.1 M sulphuric acid deuterium oxide solutions.

As E is increased from 0.15 to 1.5 V (Figs. 11 and 12) these spectra show, as expected, negative bands similar to those recorded in aqueous perchloric acid (Fig. 8). Therefore, the bands at 1620 cm^{-1} and 1110 cm^{-1} can be assigned to the formation of $TMFDS^{2+}$ and soluble gold–TMTU complex species, respectively.

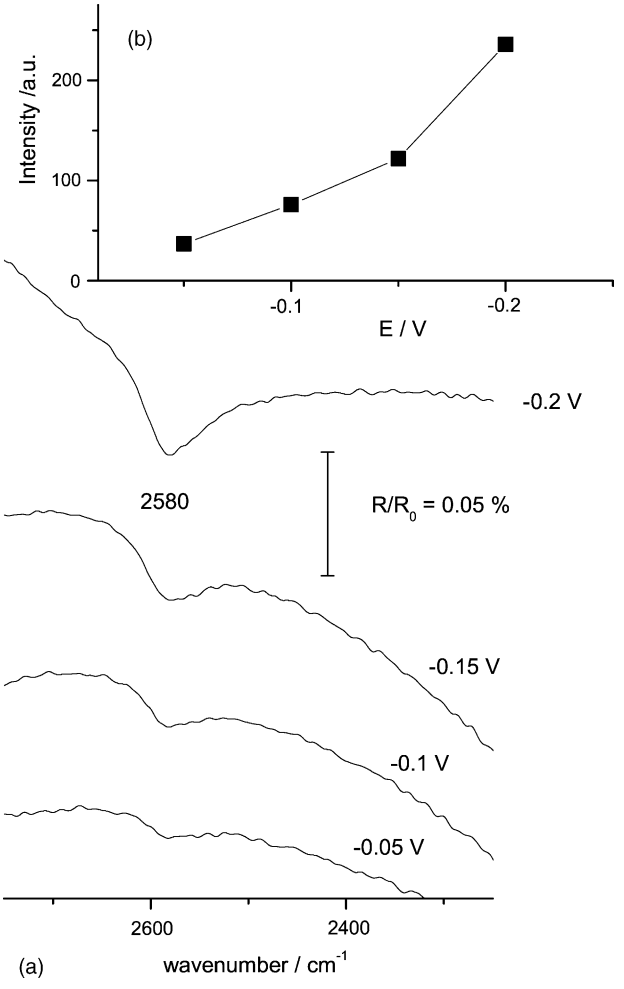

Fig. 10. (a) p-Polarised light FTIRRAS spectra recorded between 2450 and 2650 cm^{-1} for TMTU on gold in 0.1 M TMTU + 0.1 M perchloric acid at −0.2 V. (b) Dependence of the intensity of the band at 2580 cm^{-1} on E_s, $E_{ref} = 0.05$ V.

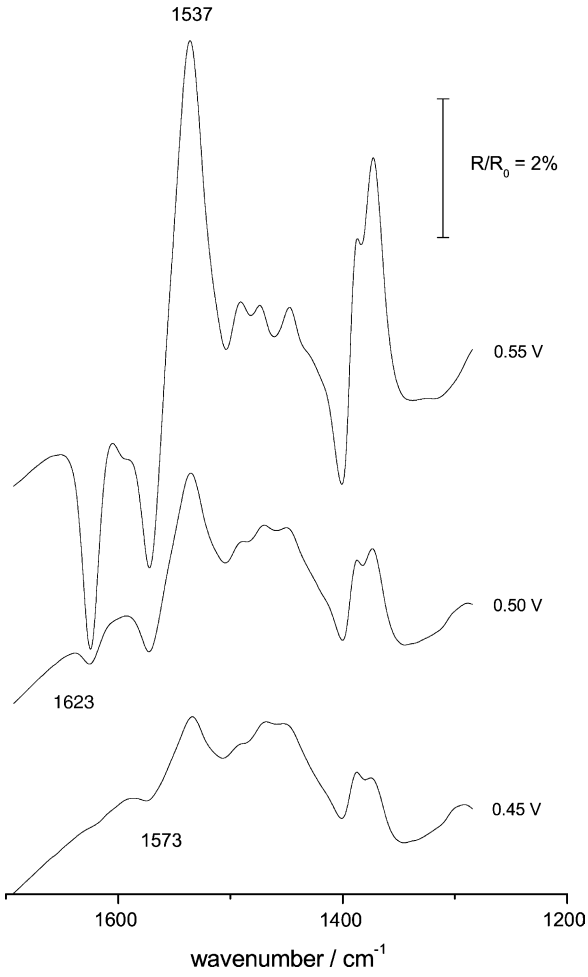

Fig. 11. p-Polarised light FTIRRAS spectra for gold in 0.1 M TMTU + 0.1 M perchloric acid in deuterium oxide recorded for sampling potentials below 0.6 V, $E_{ref} = 0.05$ V.

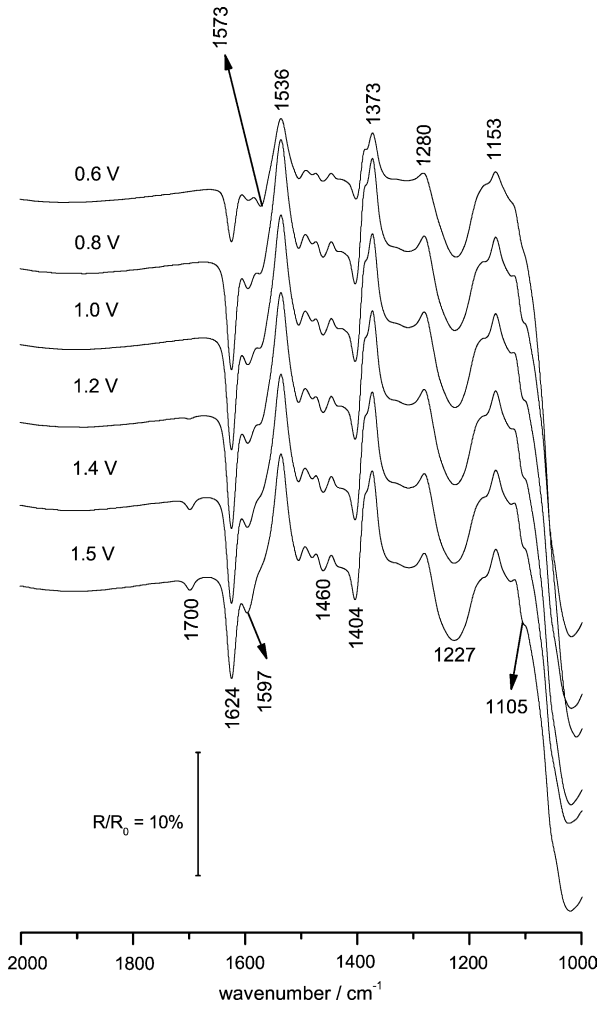

Fig. 12. *p*-Polarised light FTIRRAS spectra for the electro-oxidation of TMTU on gold in 0.1 M TMTU + 0.1 M perchloric acid in deuterium oxide at different sampling potentials, $E_{ref} = 0.05$ V.

Let us examine the spectra recorded in the range $0.4 \leq E \leq 0.55$ V where TMTU electro-oxidation to $TMFDS^{2+}$ and to soluble gold–TMTU complex ions occurs. For $E = 0.45$ V only the band at 1573 cm^{-1}, assigned to the gold–TMTU complex species, is found (Fig. 11), but when E is increased to 0.5 V the band at 1623 cm^{-1} related to $TMFDS^{2+}$ formation commences to grow, its intensity being lower than that of the band related to the formation of soluble gold–TMTU complex species. But the reversal is observed for $E = 0.55$ V. At this potential TMTU electro-oxidation turns out to be more important than TMTU-assisted gold electrodissolution.

The spectra recorded in the range $0.6 \leq E \leq 1.5$ V show the band at 1623 cm^{-1} that increases with E, and a new band at 1597 cm^{-1} that appears simultaneously with the negative band at 1400 cm^{-1}. For $E > 1.2$ V a small band at 1700 cm^{-1} is also recorded in agreement with data obtained from aqueous acid solutions (Fig. 8), albeit it should be noted that this band is much better defined in deuterium oxide solutions.

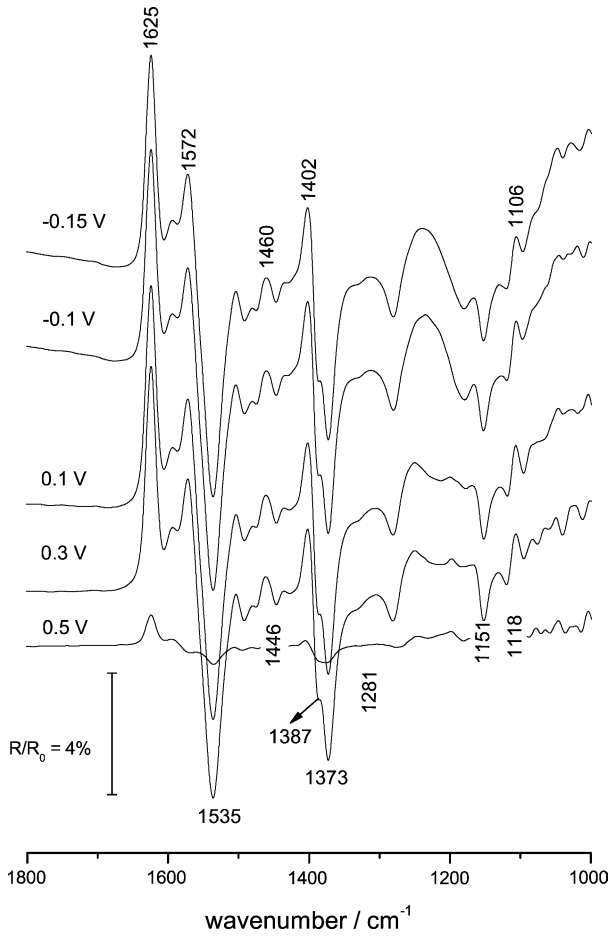

Fig. 13. *p*-Polarised light FTIRRAS spectra for TMTU on gold in 0.1 M TMTU + 0.1 M perchloric acid at different sampling potentials, $E_{ref} = 0.55$ V.

Conversely, when the electrode is initially polarised at 0.55 V, i.e. when TMTU electro-oxidation has already started, and E is subsequently decreased stepwise to −0.2 V (Fig. 13), the spectra contrast the behaviour previously described for positive increasing potentials (Section 3.5). Thus, the negative bands that appeared at 1104, 1400, 1573 and 1625 cm^{-1} (Fig. 8) now turn out to be positive. This result points out that both $TMFDS^{2+}$ and $Au(TMTU^{+})_n$ complex species are electroreduced when $E < 0.55$ V, both yielding TMTU in the thin solution layer, as indicated by the corresponding TMTU negative bands. The electroreduction of $TMFDS^{2+}$ takes place from ca. 0.5 V downwards, as denoted by the appearance of the positive band at 1623 cm^{-1}, whereas the electroreduction of the soluble TMTU-gold complex (bands at 1573 and 1106 cm^{-1}) starts at slightly more negative potentials, in agreement with data depicted in Fig. 11 for the initial stages of TMTU electro-oxidation and TMTU-assisted gold electrodissolution.

3.7. IR spectrum of solid TMFDS chloride

From the analysis of FTIRRAS data, both in aqueous and deuterated solutions, the bands appearing at 1400

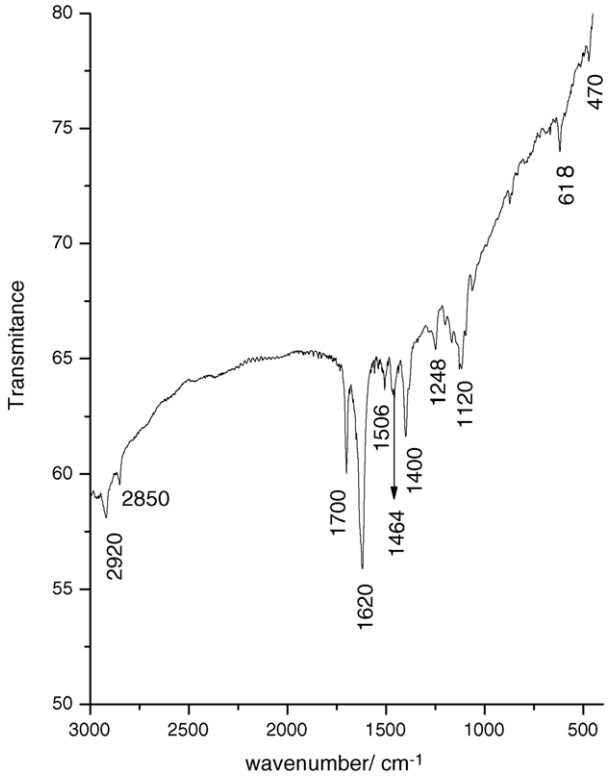

Fig. 14. IR spectrum of solid $TMFDS^{2+}$ obtained from the chemical oxidation of TMTU by hydrogen peroxide.

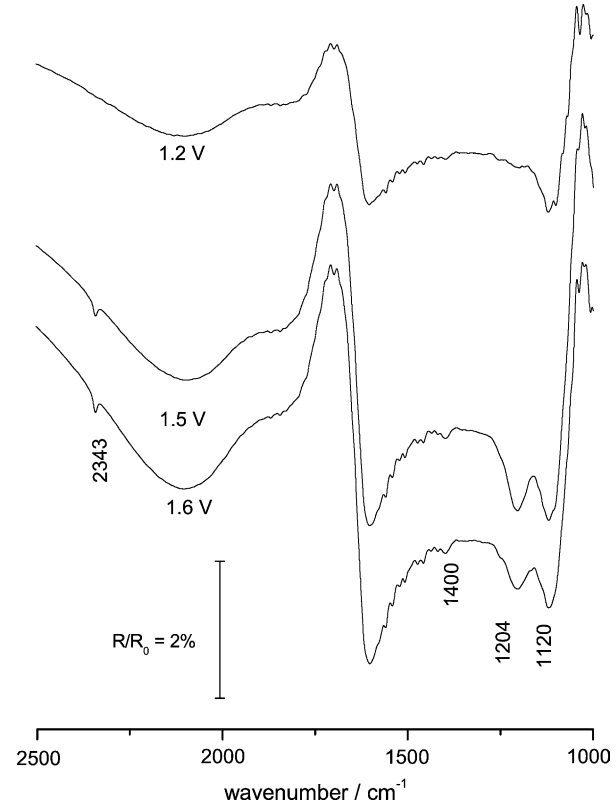

Fig. 15. *p*-Polarised light FTIRRAS spectra for the electro-oxidation of TMTU adsorbates produced at 0.05 V for 300 s. 0.1 M TMTU + 0.1 M perchloric acid at different sampling potentials, $E_{ref} = 0.05$ V.

and 1250 cm^{-1} should be related to species coming from the electro-oxidation of TMTU, and those at 1573 and 1110 cm^{-1} to soluble gold–TMTU complex species. To confirm these assignments, $TMFDS^{2+}$ chloride was produced by chemical oxidation of TMTU with hydrogen peroxide in hydrochloric acid [18,48] and the IR spectrum of the solid product recorded (Fig. 14).

It has been reported that the spectrum of $TMFDS^{2+}$ exhibits a strong band at 1610 cm^{-1} due to the CN asymmetric stretching [18], which in our case appears at 1619 cm^{-1}. The bands at 1400 and 1250 cm^{-1} are in good agreement with FTIRRAS data resulting from the electro-oxidation experiments (Fig. 8). Furthermore, the weak bands at 459 and 619 cm^{-1} can be assigned to the S–S and C–S stretching, respectively, as expected for a disulphide compound [45]. In agreement with FTIRRAS data, the bands at 1247, 1457, 1505 and 1700 cm^{-1} should be related to oxidation products from TMTU. The band at 1700 cm^{-1} indicates, as discussed above, the formation of a carbonyl-containing compound. The bands at 2850 and 2920 cm^{-1} are related to the symmetric and antisymmetric stretching of CH_3 groups [45,48].

3.8. FTIRRAS related to adsorbed TMTU electro-oxidation

The electro-oxidation of TMTU on gold produces strongly bound residues (Fig. 7) that are electro-oxidised in the potential region where the formation of the oxygen-containing layer on gold occurs. To explore the nature of these residues TMTU was adsorbed on gold from 0.1 M TMTU + 0.1 M perchloric acid for 300 s at $E_{ref} = 0.05$ V. Subsequently, the TMTU-containing solution was washed out by aqueous 0.1 M perchloric acid to run a spectrum at E_{ref}. Afterwards, E was stepped from E_{ref} to 1.2, 1.5 and 1.6 V to electro-oxidise adsorbed residues, and simultaneously, the corresponding IR spectra were recorded (Fig. 15); for $E = 1.2$ V, the spectrum shows only a negative band at 1100 cm^{-1} due to perchlorate ions. for $E = 1.5$ V and 1.6 V, the negative bands at 1200 cm^{-1} and 2343 cm^{-1} indicate the simultaneous formation of bisulphate ions and carbon dioxide, respectively. It should be noted that when E is set back from 1.6 V to $E_{ref} = 0.05$ V, the spectrum exhibits neither a positive band nor a feature related to the disappearance of methyl groups from TMTU. These results are at variance with those obtained for mono- and di-substituted thioureas that exhibit positive bands related to the symmetric and antisymmetric stretching of methyl groups [49], but are consistent with TMTU molecules adsorbed almost parallel to the electrode surface [22].

4. Discussion

Cyclic and tm-voltammetry and FTIRRAS data of TMTU dissolved in acid solutions on gold involve a series of complex

cathodic and anodic processes that occur within certain potential windows. These processes are complicated to some extent by electrosorption reactions involving either TMTU itself for $E < 0.4$ V or products from the TMTU electro-oxidation reactions for $E > 0.4$ V. Products from these reactions as well as the consumption of reactants are detected by FTIRRAS, although this technique fails to detect TMTU adsorbates probably because of the quasi-parallel orientation of the dipole moment vector of this molecule, as has been suggested from STM imaging on Au(1 1 1) [19].

For $E < 0$ V, the electroadsorptive reduction of TMTU on gold is accompanied by the discharge of hydrogen ions (Figs. 2 and 4). Conversely, in the range 0.5–0.8 V, the electro-oxidation of both adsorbed and soluble TMTU species yields $TMFDS^{2+}$ and soluble gold–TMTU complex ions. Both reactions behave as conjugated electrochemical processes, their kinetics being influenced by the amount of adsorbed residues accumulated on the electrode surface.

On the other hand, for $E > 1.4$ V, the irreversible electro-oxidation of both TMTU and $TMFDS^{2+}$ yields carbon dioxide, sulphate ions and carbonyl-containing species. The complete electro-oxidation of TMTU should also imply the formation of nitrogen as a product.

4.1. Processes in the range −0.24 to 0.20 V

In the range −0.24 to 0.20 V, the complex processes involving TMTU start by the spontaneous adsorption of TMTU on gold (see Sections 3.4 and 3.8), according to a formal reaction such as

$$n\mathrm{Au} + \mathrm{TMTU(aq)} \longrightarrow \mathrm{Au}_n(\mathrm{TMTU})_{\mathrm{ad}} \quad (1)$$

where n is the number of gold surface atoms blocked by 1 TMTU molecule. According to STM imaging [21] and adsorbate charge electro-oxidation data the average value of n (see Section 4.3, below) is $9 \leq n \leq 10$. It should be noted that at variance with TU, TMTU cannot produce a tautomeric form HS-R due to the lack of amine hydrogen, making TMTU adsorption via deprotonation unlikely.

In the absence of gold–TMTU complex species in the solution, tm-voltammetry suggests an electrosorption reaction occurring at ca. −0.18 V (Fig. 4). For $E < -0.18$ V, this reaction is produced simultaneously with the discharge of hydrogen ions yielding SH-containing TMTU residues, as inferred from FTIRRAS spectra (Fig. 10). Accordingly,

$$\mathrm{Au}_n(\mathrm{TMTU})_{\mathrm{ad}} + \mathrm{H^+(aq)} + \mathrm{e^-} \longrightarrow \mathrm{Au}_n\text{-SH-containing residues} \quad (2)$$

Reaction (2) can be related to voltammetric peaks IIa/IIc in Fig. 4. From tm-voltammetric data, it appears that reaction (2) behaves as a quasi-reversible process involving a charge density of $30 \pm 6\ \mu\mathrm{C\,cm^{-2}}$.

Furthermore, at $E < -0.18$ V, the discharge of hydrogen ions on gold partially covered by SH-containing residues would produce molecular hydrogen via hydrogen atom formation at unblocked gold sites [50]. The electro-oxidation of hydrogen formed at −0.24 V can be associated with peak IIIa at ca. 0 V in the tm-voltammograms.

As the amount of adsorbed TMTU residues produced at $E < 0$ V increases the cyclic voltammetry response in the range 0.4 to 0.9 V gradually decreases (Fig. 2a), although this effect disappears as E_{cs} is shifted to 0.05 V, i.e., the formation of adsorbed residues is then prevented.

Otherwise, in the range −0.24 to 0.20 V the capacitance of the gold|solution interface is about $10\ \mu\mathrm{F\,cm^{-2}}$, a figure smaller than that expected for the Helmholtz double layer capacitance (C_{HDL}). Accordingly, for a series arrangement of capacitors and $C_{\mathrm{HDL}} \cong 30\ \mu\mathrm{F\,cm^{-2}}$, the pseudocapacitance related to reaction (2) would result in ca. $15\ \mu\mathrm{F\,cm^{-2}}$. This figure is consistent with a small change in the local dipole moment of TMTU adsorbates on gold and, correspondingly, with the absence of adsorbate bands in FTIRRAS.

In the presence of soluble gold–TMTU complex ions (see 4.2), the cathodic reaction starting from ca. 0.4 V downwards [15] is the discharge of complex species such as

$$[\mathrm{Au(TMTU)}_n]^+ + \mathrm{e^-} \rightleftharpoons \mathrm{Au(s)} + n\mathrm{TMTU(aq)} \quad (3)$$

The electroreduction of soluble gold–TMTU complex ions results in a diffusion-controlled cathodic current that extends from 0.4 V downwards (Figs. 2a and 5a).

4.2. Processes in the range 0.40–0.95 V

The formation of gold–TMTU complex ions in the range 0.4–0.9 V occurs almost simultaneously with the electro-oxidation of TMTU producing $TMFDS^{2+}$ species.

In the potential range 0.50–0.95 V, FTIRRAS spectra show the formation of both $TMFDS^{2+}$ and soluble gold–TMTU complex ions (Fig. 8). As shown in the spectra obtained from deuterium oxide solutions (Fig. 11), when E is increased from 0.45 upwards, first gold–TMTU complex ions (band at $1573\ \mathrm{cm^{-1}}$) appear in the thin solution layer, and from $E >$ ca. 0.55 V $TMFDS^{2+}$ ions (band at $1623\ \mathrm{cm^{-1}}$) are produced. This outcome indicates that the formation of $TMFDS^{2+}$ is the dominant electrochemical process from 0.55 V upwards, whereas at lower potentials the formation of soluble gold–TMTU complex ions predominates. This conclusion is confirmed by the spectra recorded during the stepwise decrease of E from 0.55 V downwards (Fig. 13). In this case, the disappearance of $TMFDS^{2+}$ in the thin solution layer is detected before that of gold–TMTU complex ions.

On the other hand, tm-voltammetry shows another electrochemical surface process in the range 0.7–0.8 V (Fig. 4) that involves a charge density of about $50 \pm 10\ \mu\mathrm{C\,cm^{-2}}$. In this case, the potential difference of pair Ia/Ic is close to 0.120 V, as expected for an electron transfer that is still rather fast at the frequency of tm-voltammetry. The electrochemical reaction yielding soluble complex ions starts from the electrosorption equilibrium of TMTU on gold,

$$\mathrm{Au}_n(\mathrm{TMTU})_{\mathrm{ad}} \rightleftharpoons (n-1)\mathrm{Au} + \mathrm{Au(TMTU^+)_{ad}} + \mathrm{e^-} \quad (4)$$

where $Au(TMTU^+)_{ad}$ denotes a positively charged adsorbate that should be considered as a precursor of the formation of soluble gold–TMTU complex ions as E is positively shifted. The formation of these complex ions can take place according to either

$$Au(TMTU^+)_{ad} \overset{H_2O}{\rightleftharpoons} [Au(TMTU)]^+(aq) \quad (5)$$

or

$$Au(TMTU)^+_{ad} + TMTU \overset{H_2O}{\rightleftharpoons} [Au(TMTU)_2]^+(aq) \quad (6)$$

Eqs. (5) and (6) comply with the possible formation of gold–TMTU complex ions with either 1 or 2 ligands, as has been reported for other metal–TMTU complexes [23–26]. Furthermore, the gold electrodissolution pathway according to reactions (4)–(6) would involve an initial fast reversible electron transfer step that is consistent with the slope 0.060 V decade^{-1} for $E < 0.55$ V (Fig. 6b).

FTIRRAS data on deuterium oxide solutions confirm that the threshold potential for the formation of gold–TMTU complex ions is slightly smaller than that for TMTU electro-oxidation to $TMFDS^{2+}$. These results are consistent with the appearance of a common precursor (Eq. (4)) that, depending on E, leads either to a higher yield of one product or the other. Accordingly, the formation of aqueous $TMFDS^{2+}$ species can be explained assuming that the $TMTU^+$ adsorbate reacts with a TMTU molecule from the bulk of the solution

$$Au(TMTU^+)_{ad} + TMTU(aq) \longrightarrow Au(s) + TMFDS^{2+}(aq) + e^- \quad (7)$$

Experimental data (Figs. 5 and 6) indicate that reaction (7) involves a single-electron transfer step per $TMFDS^{2+}$ molecule. For $E > 0.55$ V, reaction (7) is rate-determining, as concluded from the limiting slope of 0.120 V decade^{-1}.

Therefore, the limiting anodic slopes from the $E/\log I$ plots, 0.60 and 0.120 V decade^{-1} (Fig. 6b), should be related to different dominant anodic processes. The fact that FTIRRAS flow cell experiments show no infrared bands related to the formation of $TMFDS^{2+}$ species during the electro-oxidation of adsorbed TMTU confirms that the formation of $TMFDS^{2+}$ species involves the participation of soluble TMTU molecules. Therefore, dimerisation from two neighbour TMTU molecules adsorbed on the electrode surface appears to be an unlikely explanation for $TMFDS^{2+}$ formation.

Seemingly, in the absence of TMTU in solution (Fig. 7) reaction (7) does not occur. Then, the removal of adsorbed TMTU takes place via the electro-oxidation of adsorbates starting from $E > 1.2$ V, yielding carbon dioxide and sulphate ions (Fig. 15).

4.3. Irreversible electro-oxidation process at $E > 1.2$ V

Voltammetry and FTIRRAS data show that residual soluble TMTU and $TMFDS^{2+}$ ionic species as well as their adsorbates are electro-oxidised from 1.2 V upwards. The overall electro-oxidation reaction of the TMTU molecule can be formally written as

$$((CH_3)_2N)_2CS + 14H_2O \longrightarrow 5CO_2 + N_2 + SO_4^{2-} + 40H^+ + 38e^- \quad (8)$$

where carbon dioxide and sulphate ions are determined by FTIRRAS along with some contribution of carbonyl-containing by-products (Figs. 8, 12). The latter apparently comes from the oxidation of TMTU to $TMFDS^{2+}$, as concluded from the IR spectrum of TMFDS chloride. This fact and the absence of the 1700 cm^{-1} band during adsorbate electro-oxidation for $E > 1.2$ V (Fig. 15) indicate that these byproducts come from soluble TMTU species in the thin solution layer (Fig. 8). Seemingly, at these potentials TMTU could be oxidised to tetramethylurea as the carbonyl band of urea and tetramethylurea appears in the range 1640–1700 cm^{-1} [51,52]. The formation of N_2 cannot be detected from FTIRRAS measurements, but it has been detected as a product from the electro-oxidation of thiourea on gold in acid by means of mass spectrometry measurements [53].

The voltammetric charge related to TMTU adsorbates accumulated at 0.05 V and electro-oxidised at $E > 1.2$ V is ca. 0.688 mC cm^{-2} for the first positive scan (Fig. 7). Considering that this figure involves ca. 90% of the adsorbate electro-oxidation charge, the latter can be estimated as 0.765 mC cm^{-2}. From this figure and reaction (8), the surface concentration of TMTU on gold can be estimated. Thus, as the electro-oxidation of TMTU requires 3.66×10^6 C/mol of TMTU, it results that the TMTU surface coverage on gold is about 2.09×10^{-10} mol cm^{-2}. This figure is practically the value 2.1×10^{-10} mol cm^{-2} that has been reported for TMTU adsorbed on Au (1 1 1) electrodes [21]. Furthermore, considering that one hydrogen atom would occupy one gold surface atom, it follows that one TMTU molecule should block ca. 10 gold surface atoms, in good agreement with data from STM imaging on Au(1 1 1) [21].

Carbon dioxide and sulphate ions are produced in the potential range where the oxygen-containing layer on gold is formed [35], i.e.,

$$H_2O + Au(s) \rightleftharpoons Au(OH)_{ad} + H^+(aq) + e^- \quad (9)$$

$$Au(OH)_{ad} \rightleftharpoons Au(O)_{ad} + H^+(aq) + e^- \quad (10)$$

OH and O adsorbates at the submonolayer and monolayer level resulting from reactions (9) and (10) should contribute to the electro-oxidation of both TMTU and $TMFDS^{2+}$ species.

5. Conclusions

- Electrochemical data indicate the occurrence of two redox surface processes in the potential range $-0.1 \leq E \leq -0.3$ V and $0.7 \leq E \leq 0.8$ V (versus SHE), respectively,

both related to the participation of different TMTU adsorbates.

- The absence of E-dependent IR bands and the fact that both p- and s-polarised light spectra show the same bands suggest that the TMTU molecule adsorbs almost parallel to the gold surface. The intensity of the IR bands at different E is used to follow the change in the concentration of reactants and products in the course of the reactions.
- In the range $0.4 \leq E \leq 0.8$ V both electrochemical and spectroscopic data indicate the partially competing anodic formation of soluble gold–TMTU complex ions ($E <$ 0.55 V) under diffusion control and the dominant formation of tetramethylformamidinium disulphide ions ($E >$ 0.55 V). For the latter, the polarisation curve approaches a limiting slope $\partial E/\partial \log I = 0.120$ V decade^{-1}, as would correspond to an irreversible process.
- The gold–TMTU complex cations are electroreduced at $E < 0.55$ V resulting in a cathodic limiting current under mass transport control.
- The electro-oxidation of TMTU via TMTU and TMTU derivative adsorbates takes place at $E > 1.3$ V yielding carbon dioxide and sulphate ions. These reactions involve the participation of OH adsorbates produced from water electro-oxidation on gold.
- According to FTIRRAS, in the potential range where the first step of water discharge on gold occurs, the main electro-oxidation products of soluble TMTU species are carbon dioxide, sulphate ions and carbonyl-containing species. At variance with TU, no CN-containing species are formed.
- From combined FTIRRAS and voltammetry data a more detailed interpretation of the kinetics and likely mechanism of the complex electrochemical reactions of TMTU on gold in aqueous acid solutions occurring at different potential ranges is advanced.

Acknowledgements

This work was financially supported by the Consejo Nacional de Investigaciones Científicas y Técnicas (CONICET), Agencia Nacional de Promoción Científica y Tecnológica (PICT 98 06-03251) of Argentina and the Comisión de Investigaciones Científicas de la Provincia de Buenos Aires (CICPBA). The authors are indebted to Dr. R.C.V. Piatti and Dr. J. Güida for their assistance in the preparation of $TMFDSCl_2$ and determination of its IR spectrum. AEB is member of the Research Career of CICPBA.

References

[1] D. Pletcher, F. Walsh, Industrial Electrochemistry, Chapman and Hall Ltd., London, 1990.
[2] A. Szymaszek, J. Biernat, L. Pajdowski, Electrochim. Acta 22 (1977) 359.
[3] D.F. Suarez, F.A. Olson, J. Appl. Electrochem. 22 (1992) 1002.
[4] E.E. Farndon, F.C. Walsh, S.A. Campbell, J. Appl. Electrochem. 25 (1995) 574.
[5] V.S. Martín, S. Sanllorente, S. Palmiero, Electrochim. Acta 44 (1998) 579.
[6] D.N. Upadhayay, V. Yegnaraman, Mater. Chem. Phys. 62 (2000) 247.
[7] A.E. Bolzán, I.B. Wakenge, R.C.V. Piatti, R.C. Salvarezza, A.J. Arvia, J. Electroanal. Chem. 501 (2001) 241.
[8] L.M. Gassa, J. Lambi, A.E. Bolzán, A.J. Arvia, J. Electroanal. Chem. 32 (2002) 71.
[9] G.R. Dey, D.B. Naik, K. Kishore, P.N. Moorthy, Radiat. Phys. Chem. 43 (1994) 365.
[10] G.R. Dey, D.B. Naik, K. Kishore, P.N. Moorthy, J. Chem. Soc. Perkin Trans. 2 (1994) 1625.
[11] B. Pesic, T. Seal, Metall. Trans. 21B (1990) 419.
[12] T. Kai, T. Hagiwara, H. Haseba, T. Takahashi, Ind. Eng. Chem. Res. 36 (1997) 2757.
[13] S. Aguayo Salinas, M.A. Encinas Romero, I. González, J. Appl. Electrochem. 28 (1998) 417.
[14] J. Li, J.D. Miller, Hydrometallurgy 63 (2002) 215.
[15] E. Bunge, S.N. Port, B. Roelfs, H. Meyer, H. Baumgärtel, D.J. Schiffrin, R.J. Nichols, Langmuir 13 (1997) 85.
[16] O.E. Piro, E.E. Castellano, R.C.V. Piatti, A.E. Bolzán, A.J. Arvia, Acta Cryst. C58 (2002) 252.
[17] M. Hoffmann, J.O. Edwards, Inorg. Chem. 16 (1977) 3333.
[18] U. Bierbach, W. Barklage, W. Saak, S. Pohl, Z. Naturforsch. b47 (1992) 1593.
[19] E. Bunge, R.J. Nichols, H. Baumgärtel, H. Meyer, Ber. Bunsenges. Phys. Chem. 99 (1995) 1243.
[20] O. Ikeda, H. Jimbo, H. Tamura, J. Electroanal. Chem. 137 (1982) 127.
[21] E. Bunge, R.J. Nichols, B. Roelfs, H. Meyer, H. Baumgärtel, Langmuir 12 (1996) 3060.
[22] S.N. Port, S.L. Horswell, R. Raval, D.J. Schiffrin, Langmuir 12 (1996) 5934.
[23] M. Schafer, C. Curran, Inorg. Chem. 5 (1966) 265.
[24] K.J. Wynne, P. Pearson, M.G. Newton, J. Golen, Inorg. Chem. 11 (1972) 1192.
[25] K.J. Wynne, P. Pearson, Inorg. Chem. 10 (1971) 2735.
[26] E.A.H. Griffith, G.A. Spofford, E.L. Amma, Inorg. Chem. 17 (1978) 1913.
[27] B.E. Conway, H. Angerstein-Kozlowska, F.C. Ho, J. Klinger, B. MacDougall, S. Gottesfeld, Disc. Faraday Soc. 56 (1973) 210.
[28] A.E. Bolzán, A.C. Chialvo, A.J. Arvia, J. Electroanal. Chem. 179 (1984) 71.
[29] J.O. Zerbino, N.R. de Tacconi, A.J. Arvia, J. Electrochem. Soc. 125 (1978) 1266.
[30] N.R. de Tacconi, J.O. Zerbino, A. Arvia, J. Electroanal. Chem. 79 (1977) 287.
[31] A.E. Bolzán, R.C.V. Piatti, A.J. Arvia, J. Electroanal. Chem. 552 (2003) 19.
[32] A.E. Bolzán, I.B. Wakenge, R.C. Salvarezza, A.J. Arvia, J. Electroanal. Chem. 475 (1999) 181.
[33] A.E. Bolzán, P. Schilardi, R.C.V. Piatti, T. Iwasita, A. Cuesta, C. Gutiérrez, A.J. Arvia, J. Electroanal. Chem. 571 (2004) 59.
[34] A.J. Bard, L.R. Faulkner, Electrochemical Methods, John Wiley and Sons, New York, 1980.
[35] R. Woods, A.J. Bard (Eds.), Electroanalytical Chemistry, vol. 9, Marcel Decker, New York, 1976, p. 98, Chapter 1.
[36] J. Kirchenerovâ, W.C. Purdy, Anal. Chim. Acta 123 (1981) 83.
[37] J. Stewart, J. Chem. Phys. 26 (1957) 248.
[38] R.K. Gosavi, C.N.R. Rao, J. Inorg. Nucl. Chem. 29 (1967) 1937.
[39] R.K. Gosavi, U. Agarwala, C.N.R. Rao, J. Am. Chem. Soc. 89 (1967) 235.
[40] A. Yamaguchi, P.B. Penland, S. Mizushima, T.J. Lane, C. Curran, J.V. Qualgiano, J. Am. Chem. Soc. 80 (1958) 527.
[41] U. Anthoni, P.H. Nielsen, G. Borch, J. Gustavsen, P. Klaboe, Spectrochim. Acta Part A 33 (1977) 403.

[42] T. Iwasita, F. Nart, H. Gerischer, C.W. Tobias (Eds.), Advances in Electrochemical Science and Engineering, vol. 4, VCH, Weinheim, 1995, p. 123.
[43] K. Kunimatsu, M. Samant, H. Seki, M.R. Philpott, J. Electroanal. Chem. 243 (1988) 203.
[44] A.E. Bolzán, T. Iwasita, A.J. Arvia, J. Electroanal. Chem. 554–555 (2003) 49.
[45] H. Günzler, H.-U. Gremlich, IR Spectroscopy, Wiley-VCH Verlag GmbH, Weinheim, 2002.
[46] B.E. Conway, L. Bai, Electrochim. Acta 31 (1986) 1013.
[47] L. Su, B.-L. Wu, J. Electroanal. Chem. 565 (2004) 1.
[48] A.E. Bolzán, J. Güida, O. E. Piro, E.E. Castellano, R.C.V. Piatti, A.J. Arvia, in preparation.
[49] A.E. Bolzán, T. Iwasita, A.J. Arvia, in preparation.
[50] R.C. Orellana, M.E. Martins, A.J. Arvia, Electrochim. Acta 24 (1979) 469.
[51] X. Otte, B. Eurard, L. Oelattre, L. Thunus, Anal. Chim. Acta 451 (2002) 323.
[52] V. Climent, A. Rodes, J. Orts, A. Aldaz, J. Feliu, J. Electroanal. Chem. 461 (1999) 65.
[53] G. Garcia, J.L. Rodriguez, G.I. Lacconi, E. Pastor, Langmuir 20 (2004) 8773.